Supporting Information

Rahmeh et al. 10.1073/pnas.1013559107

SI Materials and Methods

Recombinant Protein Expression. Plasmids carrying functional VSV L and P genes were described previously (1). Fragments of L were amplified from the L gene and confirmed by sequencing. A hexahistidine (6× His) tag was introduced at the N terminus of L and one set of L fragments (Table S1). In a second set, the L fragments were inserted in frame of a 6× His-SUMO* tag described in ref. 2 (Table S1). The genes were inserted into pFASTBAC DUAL vector (Invitrogen) under control of the polyhedrin promoter as described previously (3). Recombinant baculovirus (BV) were recovered following transfection of bacmid DNA into *Spodoptera frugiperda* Sf21 cells using Cellfectin (Invitrogen). The recombinant BVs were amplified and used to infect Sf21 cells growing in spinner flasks at 1.5×10^6 cells/mL at a multiplicity of infection (MOI) of 3–5. The cells were collected at 65–72 h postinfection. Protein expression was evaluated by Western blot with an anti-His monoclonal antibody (Clontech).

P was cloned downstream of the His tag of a pET–16b vector (Novagen). The plasmid was transformed in BL21 (DE3) *Escherichia coli*. The cells were grown in LB containing 100 μg/mL ampicillin and induced at A_{600} of 0.6 with 1 mM isopropyl β-D-thiogalactopyranoside (IPTG) at 30 °C for 4 h.

Purification of L Fragments. All fragments were first purified using Ni-NTA agarose chromatography (Qiagen), as described previously for full-length L and eluted in 50 mM NaH_2PO_4 pH 7.4, 300 mM NaCl, 200 mM Imidazole (3). Peak fractions were diluted in an equal volume of buffer A (50 mM Tris-HCl pH 7.0, 10% glycerol, 1 mM DTT). Fragments 1–1,593, 1–1,114, and 1–860 were individually loaded on a Mono S 5/50 GL column (GE Healthcare) equilibrated with buffer A containing 150 mM NaCl. The column was washed with five column volumes (CV) of equilibration buffer and eluted with a 10 CV continuous gradient of 150 mM to 1 M NaCl in buffer A. Fragment 1,594–2,109 was first loaded on a similarly equilibrated Mono Q 5/50 GL column (GE Healthcare) and collected from the flow through, then subsequently purified on the Mono S column as described for the other fragments.

Electron Microscopy Image Collection and Processing. The 60°/0° image pairs for full-length L and the L–P complex or only images of untilted specimens for all of the other samples were collected with a Tecnai T12 electron microscope (FEI) equipped with an LaB_6 filament and operated at an acceleration voltage of 120 kV. Images were recorded on imaging plates at a magnification of 67,000× and a defocus of about −1.5 μm using low-dose procedures. Imaging plates were read out with a scanner (DITABIS) using a step size of 15 μm, a gain setting of 20,000, and a laser power setting of 30%; 2 × 2 pixels were averaged to yield a pixel size of 4.5 Å at the specimen level (4). Class averages and 3D reconstructions were calculated using the SPIDER software package (5). BOXER, part of the EMAN software package (6), was used to interactively select particles from images of the L fragments. For the 1–1,593 fragment, 8,874 particles were selected from 112 images and windowed into 64 × 64-pixel images. For the 1,594–2,109 fragment, 12,888 particles were selected from 56 images and windowed into 44 × 44 pixel images. For the 1–1,114 fragment, 15,954 particles were selected from 40 images and windowed into 50 × 50 pixel images. For the 1–860 fragment, 10,518 particles were selected from 80 images and windowed into 50 × 50 pixel images. The particles in the data sets were classified using the SPIDER software package (5). The particles were rotationally and translationally aligned and subjected to 10 cycles of multireference alignment. Each round of multireference alignment was followed by *K*-means classification into 50 classes. The references used for the first multireference alignment were randomly chosen from the particle images.

For full-length L, 9,905 pairs of particles (8,806 single and 1,099 double particles) were selected from 108 60°/0° tilt pairs using WEB, which is part of the SPIDER software package, windowed into 120 × 120 pixel images, and the particles selected from the untilted specimen were classified into 50 classes (single particles) or 10 classes (double particles) as described above. For the L–P complex, 8,665 pairs of particles (5,885 single and 2,780 double particles) were selected from 217 60°/0° tilt pairs using WEB, windowed into 120 × 120 pixel images, and the particles selected from the untilted specimen were classified into 50 classes (single particles) or 20 classes (double particles) as described above. A total of 44 of the classes for the single species of L and 17 of the classes for the single species of the L–P complex were selected to calculate individual 3D reconstructions using the corresponding particles selected from the tilted specimen. The 3D reconstructions were generated by using the back-projection and angular refinement procedures implemented in SPIDER and visualized using DNG from the OpenStructure framework (7). Selected 3D reconstructions showing the structural features seen in the respective class averages are presented in Fig S2.

In Vitro Transcription. The mRNAs were synthesized in vitro using 5 μg of N–RNA template, 0.5 μg of P, and 1 μg of L or (1 μg of 1–1,593 + 1 μg of 1,594–2,019) or 1.5 μg of the S200 peak fraction for the L–P complex. Reactions were performed in the presence of 1 mM ATP; 0.5 mM CTP, GTP, and UTP; 15 μCi of [α-^{32}P] GTP (PerkinElmer), 30% vol/vol rabbit reticulocyte lysates (Promega), 0.05 μg/μL actinomycin D (Sigma) in transcription buffer [30 mM Tris-HCl pH 8.0, 33 mM NH_4HCl, 50 mM KCl, 4.5 mM $Mg(OAC)_2$, 1 mM DTT, 0.2 mM spermidine, 0.05% Triton X-100]. Reactions included 1 mM of the MTase inhibitor S-adenosyl homocysteine (SAH) (Sigma) where indicated. The products were purified by phenol/chloroform extraction, separated by acid-agarose urea gel electrophoresis as previously described (3). and visualized using a PhosphorImager (GE Healthcare).

Tobacco Acid Pyrophosphatase (TAP) Digestion. A total of 50 ng of purified RNA from in vitro transcription reactions performed in the absence or presence of 1 mM SAH were digested with 1 U of TAP (Epicenter) in 10 μL TAP reaction buffer (50 mM sodium acetate pH 5.0, 1 mM EDTA, 0.1% β-mercaptoethanol and 0.01% Triton X-100) at 37 °C for 2 h, and the products were analyzed by TLC on PEI-F cellulose sheets (EM Biosciences) using 1.2 M LiCl as solvent as described previously (8). Spots were visualized using a PhosphorImager (GE Healthcare). Markers 7^mGp and Gp were visualized by UV shadowing at 254 nm.

Preparation of Total Cell Extracts Expressing eGFP–P. Plasmid peGFP–P was created by cloning the eGFP–P ORF from the previously described recombinant vesicular stomatitis virus (9) into the T7 expression vector pGEM3 (Promega). Confluent 6-cm dishes with 2×10^6 BSR-T7 cells were infected at an MOI of 3 with recombinant vaccinia virus (vTF73) expressing T7 RdRP (10). After 1 h, cells were washed and transfected with 3.8 μg peGFP–P plasmid using Lipofectamine 2000 standard protocol (Invitrogen) and harvested at 24 h. Total cell extracts were prepared by lysing

cells in lysis buffer containing 10 mM Tris-HCl pH 7.4, 150 mM NaCl, 1% Nonidet P-40, 0.5% sodium deoxycholate, 0.1% SDS and 10 mM imidazole. The lysates were clarified by centrifugation at 10,000 *g* for 20 min at 4 °C.

Ni-NTA Pulldown Assay. A total of 300 μg of total cell lysates expressing eGFP–P were incubated with 2 μg of 6× His-tagged L or 1–1,593, 1,594–2,109, (2 μg of 1–1,593 + 2 μg of 1,594–2,019 preincubated on ice for 1 h) or 2 μg of the N-terminal domain of anthrax lethal factor as control and 15 μL of Ni-NTA agarose beads (Qiagen) at 4 °C for 1 h. The beads were precipitated by centrifugation at 2,000 × *g* for 3 min and washed five times with 500 μL of lysis buffer containing 30 mM imidazole. The beads were boiled in 2× SDS/PAGE loading buffer and the proteins were separated by 10% SDS/PAGE.

1. Pattnaik AK, Wertz GW (1990) Replication and amplification of defective interfering particle RNAs of vesicular stomatitis virus in cells expressing viral proteins from vectors containing cloned cDNAs. *J Virol* 64:2948–2957.
2. Liu L, Spurrier J, Butt TR, Strickler JE (2008) Enhanced protein expression in the baculovirus/insect cell system using engineered SUMO fusions. *Protein Expr Purif* 62: 21–28.
3. Li J, Rahmeh A, Morelli M, Whelan SP (2008) A conserved motif in region V of the large polymerase proteins of nonsegmented negative-sense RNA viruses that is essential for mRNA capping. *J Virol* 82:775–784.
4. Li Z, Hite RK, Cheng Y, Walz T (2010) Evaluation of imaging plates as recording medium for images of negatively stained single particles and electron diffraction patterns of two-dimensional crystals. *J Electron Microsc (Tokyo)* 59:53–63.
5. Frank J, et al. (1996) SPIDER and WEB: Processing and visualization of images in 3D electron microscopy and related fields. *J Struct Biol* 116:190–199.
6. Ludtke SJ, Baldwin PR, Chiu W (1999) EMAN: Semiautomated software for high-resolution single-particle reconstructions. *J Struct Biol* 128:82–97.
7. Biasini M, et al. (2010) *OpenStructure: A Flexible Software Framework for Computational Structural Biology* (Bioinformatics, Oxford, England).
8. Li J, Fontaine-Rodriguez EC, Whelan SP (2005) Amino acid residues within conserved domain VI of the vesicular stomatitis virus large polymerase protein essential for mRNA cap methyltransferase activity. *J Virol* 79:13373–13384.
9. Schott DH, Cureton DK, Whelan SP, Hunter CP (2005) An antiviral role for the RNA interference machinery in *Caenorhabditis elegans*. *Proc Natl Acad Sci USA* 102: 18420–18424.
10. Fuerst TR, Niles EG, Studier FW, Moss B (1986) Eukaryotic transient-expression system based on recombinant vaccinia virus that synthesizes bacteriophage T7 RNA polymerase. *Proc Natl Acad Sci USA* 83:8122–8126.

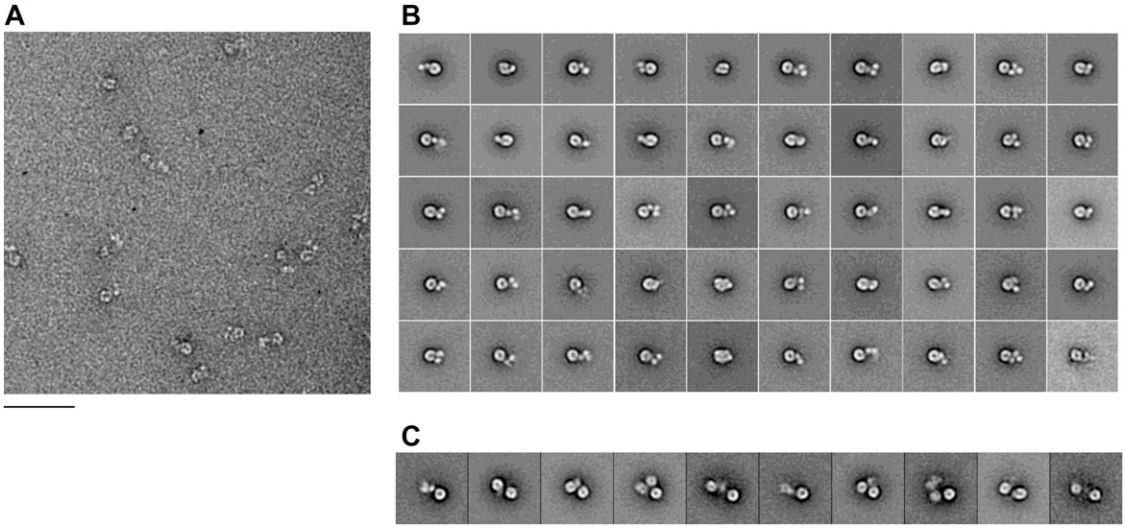

Fig. S1. Single particle analysis of L. (*A*) Representative EM image of L in negative stain. (Scale bar: 50 nm.) (*B*) Class averages of L singles obtained by classification of 8,806 particles into 50 classes. (*C*) Class averages of L doubles obtained by classification of 1,099 particles into 10 classes. The side length of the individual panels in *B* and *C* is 54 nm.

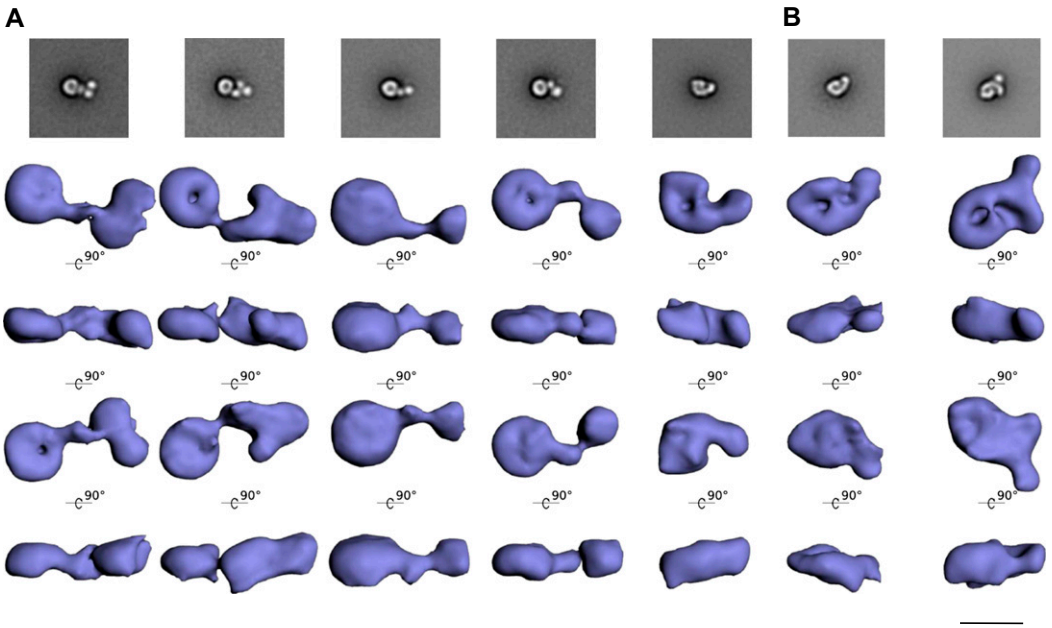

Fig. S2. The 3D reconstructions of L and the L–P complex. Class averages and corresponding 3D reconstructions of (*A*) L and (*B*) the L–P complex in negative stain. Different views of each reconstruction are shown rotated by 90° about the horizontal axis as indicated by the arrows. (Scale bar: 10 nm.) The 3D reconstructions are consistent with the respective class averages, revealing the ring-shaped core domain and the appendage. Due to flattening of the particles introduced by the negative staining procedure and the limited resolution of the density maps, potentially due to remaining structural heterogeneity within individual classes of particles, the 3D maps do not provide more information than the projection averages. In particular, the density maps of L and the L–P complex do not have sufficient structural detail to reveal the conformational change that occurs in the appendage of L upon binding of P.

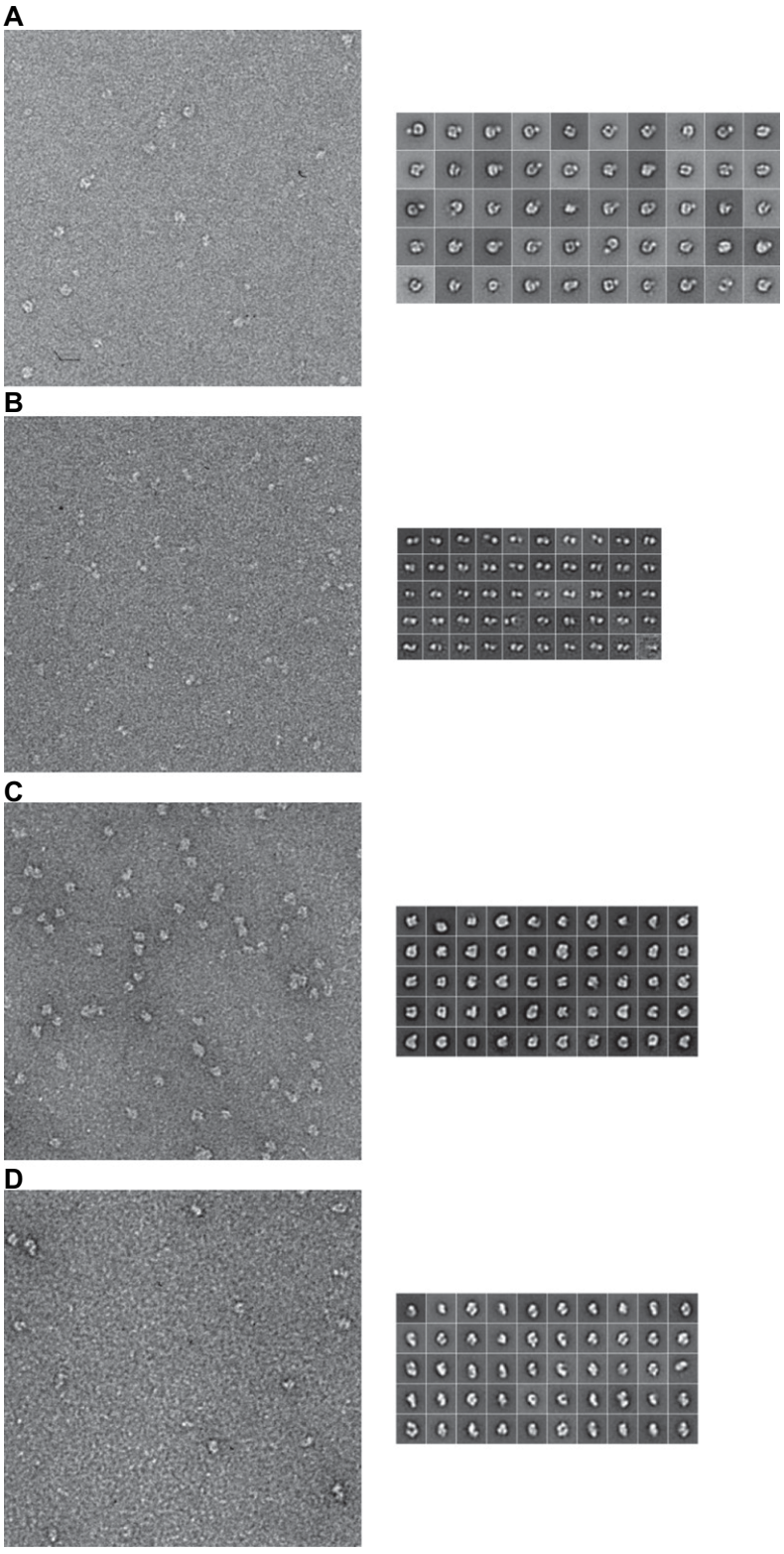

Fig. S3. Single-particle EM analysis of negatively stained L fragments. *Left* shows representative EM images (Scale bar: 50 nm) and *Right* shows the 50 class averages for (*A*) the 1–1,593 fragment, for which the side length of the individual panels is 29 nm, (*B*) the 1,594–2,109 fragment, for which the side length of the individual panels is 20 nm, (*C*) the 1–1,114 fragment, for which the side length of the individual panels is 22 nm, and (*D*) the 1–860 fragment, for which the side length of the individual panels is 22 nm.

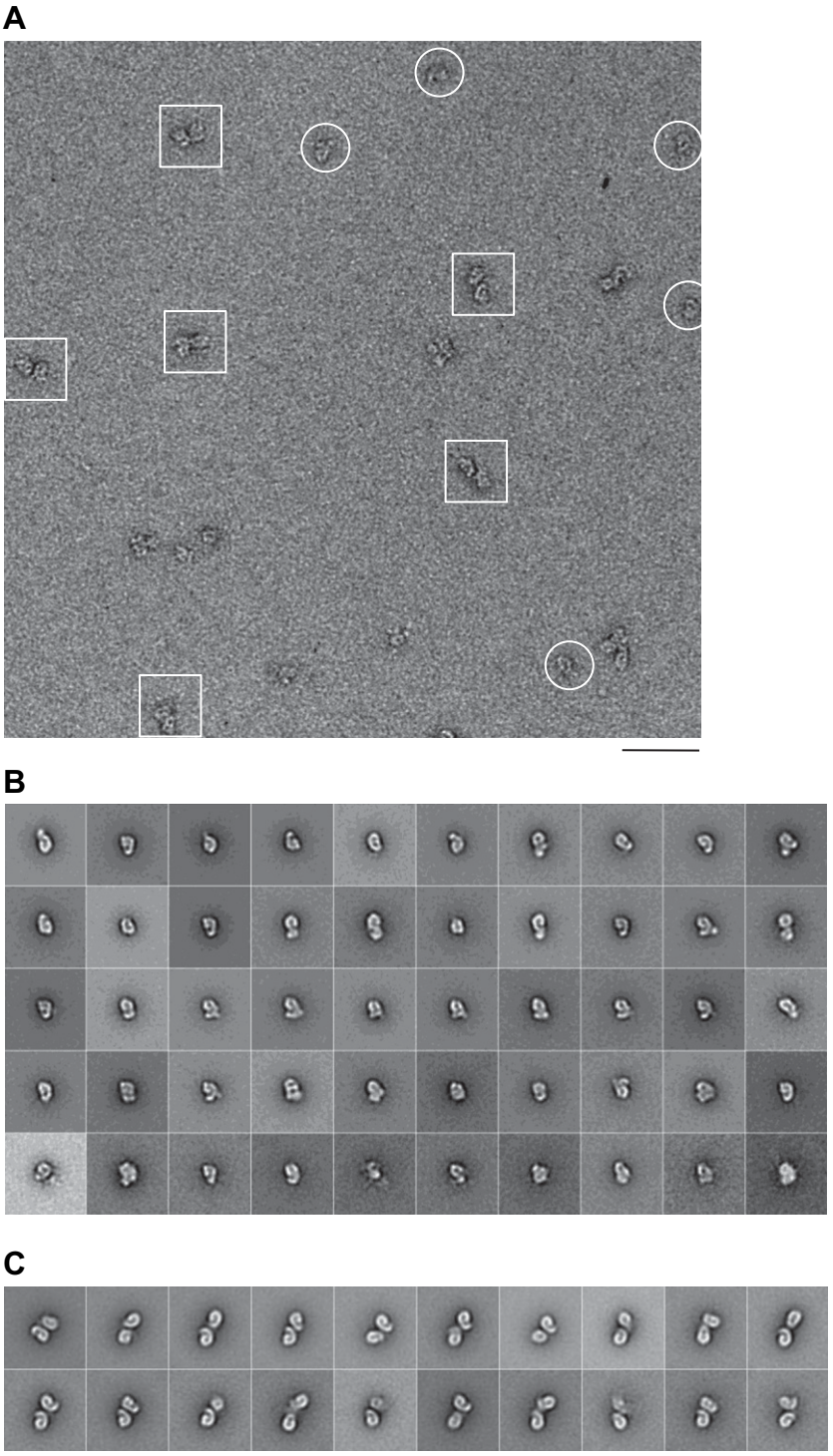

Fig. S4. Single-particle EM analysis of negatively stained L–P complex. (*A*) Representative EM image of the L–P complex with single particles indicated by white circles and double particles by white squares. (Scale bar: 50 nm.) (*B*) Class averages of single L–P particles obtained after classification of 5,885 particles into 50 classes. (*C*) Class averages of double L–P particles obtained after classification of 2,780 particles into 20 classes. The side length of the individual panels in *B* and *C* is 54 nm.

Table S1. Summary of designed VSV L fragments

Construct	Expression
(*i*) N–His	
1–2,109	+++
1–860	+++
1–1,045	+
1–1,080	–
1–1,114	++
1–1,254	+
1–1,378	+
1–1,498	–
1–1,560	–
1–1,593	++
861–2,109	–
1,046–2,109	–
1,594–2,109	+++
1,046–1,593	–
1,594–1,860	+
100–1,593	–
261–1,593	–
1,255–2,109	–
(*ii*) N–His–SUMO*	
194–2,109	–
304–2,109	–
341–2,109	–
413–2,109	–
588–2,109	–
599–2,109	–
861–2,109	–
920–2,109	–
941–2,109	–
1,046–2,109	–
1,070–2,109	–
1,332–2,109	±
1,378–2,109	±
1,476–2,109	–

Full-length L (1–2,109) and fragments were expressed in insect cells as (*i*) N–His-tagged or (*ii*) N–His–SUMO*-tagged. Expression levels are marked from highest (+++) to lowest (–).